Redox Biology 39 (2021) 101835

Contents lists available at ScienceDirect

Redox Biology

journal homepage: www.elsevier.com/locate/redox

Research Paper

Context-dependent responses of *Drosophila* intestinal stem cells to intracellular reactive oxygen species

Fei Chen [1], Run Su [1], Shiwei Ni, Yan Liu, Jiexiang Huang, Gege Li, Qun Wang, Xi Zhang, Yufeng Yang [*]

Institute of Life Sciences, Fuzhou University, Fuzhou, Fujian Province, 350108, China

ARTICLE INFO

Keywords:
Reactive oxygen species
Drosophila
Intestinal stem cell
Tumor
Notch
Integrin

ABSTRACT

Reactive oxygen species (ROS) contribute to cellular redox environment and serve as signaling molecules. Excessive ROS can lead to oxidative stress that are involved in a broad spectrum of physiological and pathological conditions. Stem cells have unique ROS regulation while cancer cells frequently show a constitutive oxidative stress that is associated with the invasive phenotype. Antioxidants have been proposed to forestall tumor progression while targeted oxidants have been used to destroy tumor cells. However, the delicate beneficial range of ROS levels for stem cells and tumor cells under distinct contexts remains elusive. Here, we used *Drosophila* midgut intestinal stem cell (ISCs) as an *in vivo* model system to tackle this question. The ROS levels of ISCs remained low in comparison to that of differentiated cells and increased with ageing, which was accompanied by elevated proliferation of ISCs in aged *Drosophila*. Neither upregulation nor downregulation of ROS levels significantly affected ISCs, implicating an intrinsic homeostatic range of ROS in ISCs. Interestingly, we observed similar moderately elevated ROS levels in both tumor-like ISCs induced by *Notch* (*N*) depletion and extracellular matrix (ECM)-deprived ISCs induced by β-integrin (*mys*) depletion. Elevated ROS levels further promoted the proliferation of tumor-like ISCs while reduced ROS levels suppressed the hyperproliferation phenotype; on the other hand, further increased ROS facilitated the survival of ECM-deprived ISCs while reduced ROS exacerbated the loss of ECM-deprived ISCs. However, *N*- and *mys*-depleted ISCs, which resembled metastatic tumor cells, harbored even higher ROS levels and were subjected to more severe cell loss, which could be partially prevented by ectopic supply of antioxidant enzymes, implicating a delicate pro-surviving and proliferating range of ROS levels for ISCs. Taken together, our results revealed stem cells can differentially respond to distinct ROS levels under various conditions and suggested that the antioxidant-based intervention of stem cells and tumors should be formulated with caution according to the specific situations.

1. Introduction

Reactive oxygen species (ROS) are proposed to play a key role in regulating stem cell homeostasis. A low intracellular concentration of reactive oxygen species (ROS) is emerging as a critical condition for stemness and pluripotency in several self-renewing tissues [1–6]. A moderate increase in ROS can promote cell proliferation and differentiation [7–9], whereas excessive amounts of ROS can cause oxidative damage to lipids, proteins and DNA [10]. However, the delicate beneficial range of ROS levels for stem cells to survive and proliferate remains elusive.

Elevated oxidative status has been found in cancer cells compared with their normal counterparts, which contribute to carcinogenesis [11–13]. Animal studies using either gene knockout or transgenic overexpression approaches demonstrated a potential role for antioxidant molecules as tumor suppressors [14–16]. If the levels of ROS reaches a certain threshold, ROS may exert a cytotoxic effect [17]. Accordingly, antioxidant supplement could actually be beneficial for tumor cells and stimulate tumor growth [18]. However, little is known about the impact of distinct endogenous ROS levels on tumor cells.

Despite the advances in clinical and preclinical trials of cancer therapy, tumor metastasis is still a key target for any anti-cancer strategies and the leading cause of death of cancer patients. Tumor metastasis is a complicated progress including EMT, migration, invasion of the

* Corresponding author.
E-mail address: yangyf@fzu.edu.cn (Y. Yang).
[1] These authors contributed equally.

https://doi.org/10.1016/j.redox.2020.101835
Received 9 October 2020; Received in revised form 26 November 2020; Accepted 13 December 2020
Available online 17 December 2020

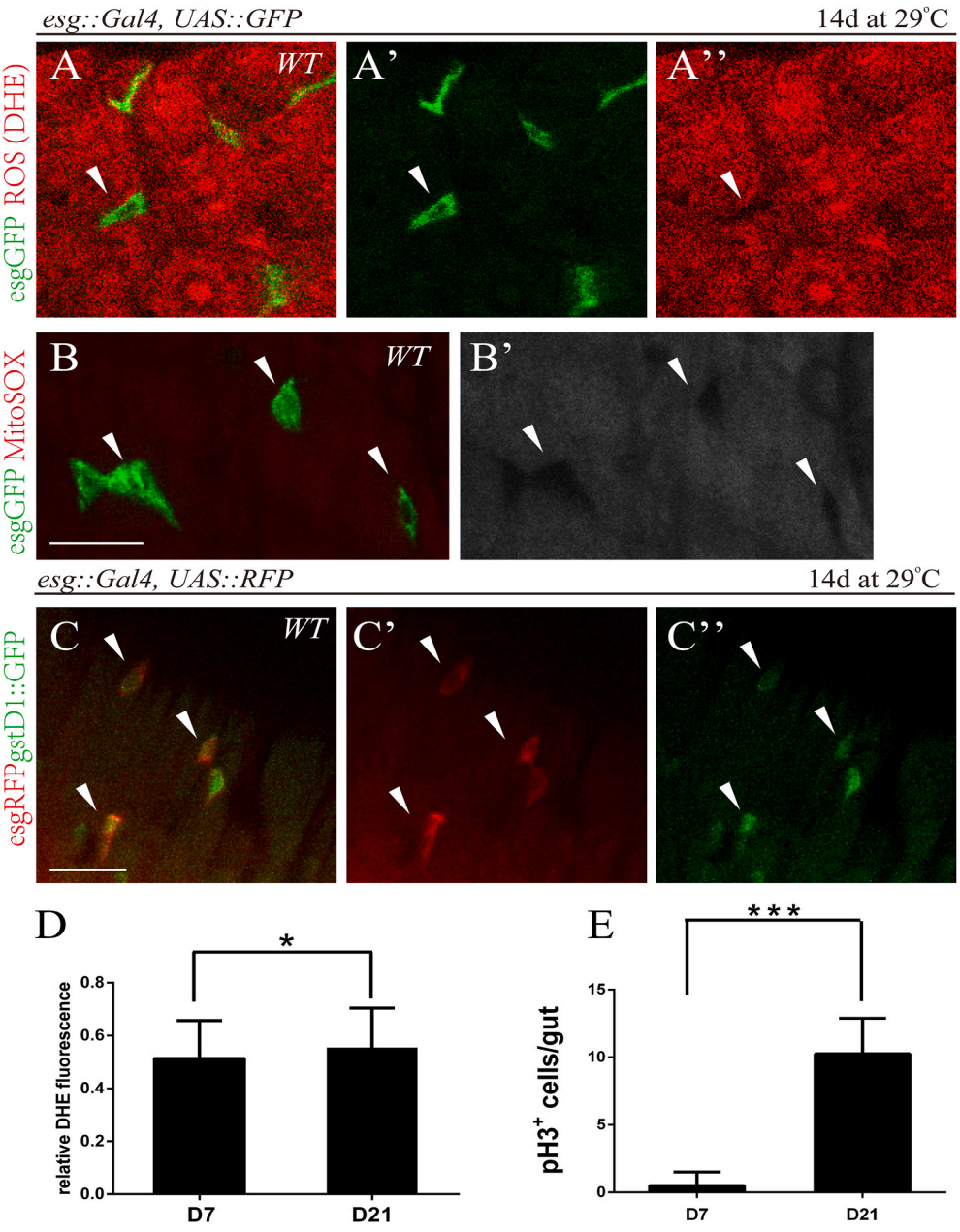

Fig. 1. The ROS levels of ISCs remained low and increased with ageing

(A, B) Relatively lower ROS levels in ISCs in comparison to neighboring differentiated EC cells. Intestines from flies (control, "*WT*") carrying *esg-Gal4, UAS-GFP* (ISC/EB marker; A′, green) were stained for DHE (A) or MitoSOX (B). White arrowheads indicate low levels of DHE (red, A″) and MitoSOX (red, B′) in ISCs. Scale bars, 20 μm. (C) Pronounced *gstD:GFP* signal in ISCs in comparison to neighboring differentiated EC cells. Intestines from flies carrying the *gstD::GFP* reporter and *esg-Gal4, UAS-RFP* (ISC/EB marker; red). RFP (C′) and GFP (C″) staining are shown separately. Note colocalization of RFP and GFP expression (white arrowheads point to the colocalization), indicating that CncC activity is present in ISCs. Scale bars, 20 μm. (D) Elevated ROS levels in ISCs of older fruit flies. The fluorescence intensity of the DHE channel was calculated using Metamorph software. Relative DHE fluorescence in ISCs was normalized to DHE fluorescence in adjacent ECs. Quantifications of relative DHE fluorescence in intestines of 7- and 21-day-old flies are shown (average and SEM; Student's *t*-test and Mann-Whitney test. *, $P < 0.05$; **, $p < 0.01$; ***, $p < 0.001$; ****, $P < 0.0001$ here and for all figures). (E) Increased proliferative capacity of ISCs in older fruit flies. Amounts of $pH3^+$ cells in intestines of 7- and 21-day-old flies are shown (average and SEM; Student's *t*-test and Mann-Whitney test). (For interpretation of the references to colour in this figure legend, the reader is referred to the Web version of this article.)

tumor cells and angiogenesis around the tumor lesion. It is worth noting that redox alterations in different states of cancer progression are also very complicated. Recently, the involvement of ROS signaling in tumor metastasis was highlighted [19]. The increased ROS stress in cancer cells has a pivotal role in the acquisition of epithelial-mesenchymal transition and metastasis [20,21]. However, ROS levels in different stages of cancer progression remains largely unknown. Understanding the redox alteration precisely may help in the battle against cancer.

The adult *Drosophila* midgut is advantageous for studies of stem cell behavior, tissue homeostasis, aging, and cancer [22–25] as it has similarities in genetic regulation and cellular composition with mammalian digestive systems [26,27]. The *Drosophila* midgut is maintained by multipotent intestine stem cells (ISCs) that give rise to enteroblasts (EBs), which in turn differentiate into either enterocytes (ECs) or enteroendocrine cells (EEs) [28,29]. Establishment and maintenance of the *Drosophila* gut epithelium require strict control of ISC proliferation and differentiation. Disruption of this cellular homeostasis can cause abnormal gut functionalities, such as tumor growth [30,31]. Overall, these features provide a unique opportunity to combine the power of *Drosophila* genetics and the simplicity of this adult homeostatic tissue to study the role of ROS under physiological and pathological conditions.

Notch (*N*) is essential for lineage differentiation and disruption of *N* in ISCs results in accumulation of ISC-like cells, which eventually develop into tumor-like masses [28,32]. Based on this, we generated ISC tumor model by suppressing *Notch* signaling [25]. By using *in vivo* imaging, we observed tumor formation, wherein intracellular ROS levels in ISCs were moderately increased. Meanwhile, ectopic providing oxidant scavenging enzymes could limit tumor growth in this model, suggesting that intracellular redox balance of ISCs influence the rate of stem cell proliferation.

Genes relevant to EMT and metastasis include integrin [20], which is the main cellular adhesion receptor implicated in nearly every step of cancer progression from primary tumor development to metastasis. Altered integrin expression is frequently detected in tumors [33]. In the *Drosophila* intestine, βPS integrin subunits (encoded by the gene myospheroid, *mys*) are critical for both maintenance and proliferation of ISCs

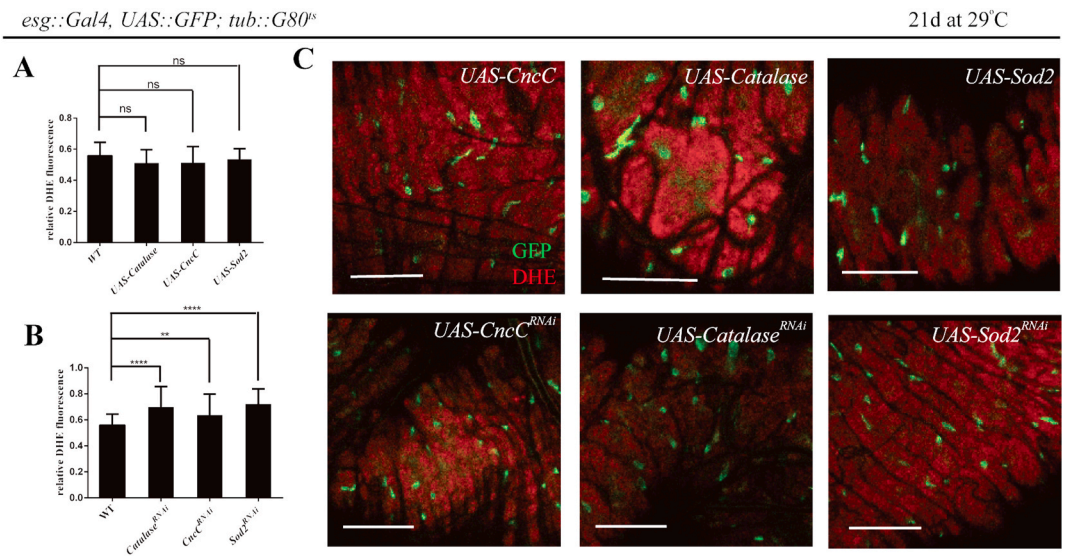

Fig. 2. Perturbation of ROS in ISCs barely disrupted the intrinsic homeostasis under physiological condition.
(A) No significant difference in ROS levels in ISCs between flies with overexpressed ROS-scavenging enzymes and those in control. Quantifications of relative DHE fluorescence of intestines overexpressing CncC, Catalase and Sod2 at 29 °C for 21 days are shown (average and SEM; ANOVA test). Relative DHE fluorescence in ISCs was normalized to DHE fluorescence in adjacent ECs. ns, not significant. (B) Significant increase in ROS levels by ROS-scavenging enzymes knockdown in ISCs. Quantifications of relative DHE fluorescence of intestines expressing Catalase^{RNAi}, CncC^{RNAi}, and SOD2^{RNAi} at 29 °C for 21 days are shown (average and SEM; ANOVA test). Relative DHE fluorescence in ISCs was normalized to DHE fluorescence in adjacent ECs. Transgenes was induced by shifting flies to restrictive temperature (29 °C). Intestines were analyzed 21 days after induction. (C) Representative confocal images of posterior midgut in flies of indicated genotypes in (A and B). DHE staining of intestines expressing CncC, Catalase and SOD2 or expressing Catalase^{RNAi}, CncC^{RNAi}, and SOD2^{RNAi} by esg-Gal4 via the TAEGET system. Scale bars, 50 μm.

(Lin et al.). We showed that *mys*-depleted ISCs had the similarly moderate elevation of ROS levels as *N*- depleted ISCs, which was accompanied by ISCs loss. Furthermore, we depleted both *N* and *mys* to mimic ECM-deprived tumor model. Strikingly, tumor cells that surviving without their natural ECM niches, exhibited the extraordinarily high ROS levels, and antioxidant treatments increased the surviving rate. Taken together, our results implicate that ROS plays a key role in the regulation of ISC, and demonstrated that there are distinct ROS levels under different cellular states and differential responses of stem cells or tumor cells to antioxidant treatments in different contexts.

2. Experimental procedures

2.1. Fly lines and husbandry

The following fly stocks were used: The wild type *D. melanogaster* flies used in this study were w^{1118} (Bloomington no. 5905), y^1,w^1; *esg::Gal4, UAS::GFP; tub::Gal80*, y^1,w^1; *esg::Gal4, UAS::RFP; tub::Gal80*, *gstD1::GFP,* RNAi transgenes: *UAS-Notch-RNAi* (Bloomington no. 7078), *UAS-CncC-RNAi* (Bloomington no. 32863), *UAS-Catalase-RNAi* (Bloomington no. 34020), *UAS-Sod2-RNAi* (Bloomington no. 32496), and UAS-Sod2 (Bloomington no. 24494) was obtained from Bloomington *Drosophila* stock center. UAS-mys-RNAi (VDRC-29619) was obtained from Vienna Drosophila RNAi center; The UAS cncC, *UAS-Catalase* was a gift from Prof. D. Bohmann (University of Rochester, NY, USA). Flies were reared on yeast/molasses-based food at 25°Cwith a 12 h light/dark cycle unless otherwise noted. Food was changed every 3–4 days.

2.2. TARGET system and temperature shifting

The TARGET system was used for temporal and spatial control of transgene expression in adult flies. Flies were reared at 18 °C. Progeny were allowed to emerge and then shifted to new vials with fresh food 1–2 days after eclosion and kept in the restrictive temperature of 29 °C incubators before dissection unless specified.

2.3. In vivo detection of ROS via DHE and MitoSOX^{TM}

ROS levels were detected in live tissue as described (Owusu-Ansah et al., 2008). Guts were dissected and handled throughout in PBS medium. After incubation in 30 mM DHE (Invitrogen)/MitoSOX^{TM} for 7/10 min in the dark at 25 °C/37 °C, guts were washed three times with PBS medium and mounted. Images were captured immediately via confocal microscopy (488/543 nm excitation, 510–540/550–610 nm detection, fixed laser power, gain and offset settings). Z-series spanning the intestinal epithelium of posterior midgut were collected and single confocal sections were used to measure signal intensities with the region measure in Metamorph software. ISCs were identified by their esgGFP expression, their size, and their basal location within the intestinal epithelium. Where possible, only isolated esgGFP$^+$ cells were measured.

2.4. Immunofluorescence

The intestines were dissected in Insect Medium. Gut fixation and immunostraining were as previously described (Linetal.,2008). Following antisera and dyes were used: rabbit anti-phospho-Histone H3 antibody (Cell signaling, 1:1000); mouse anti-GFP antibody (Invitrogen, 1:1000); Alexa-488-conjugated goat anti-mouse secondary antibodies and Alexa-568-conjugated goat anti-rabbit secondary antibodies (Invitrogen, 1:1000); DAPI (49,69-diamidino-2-phenylindole, Sigma; 0.1 mg/ml, 5 min incubation). Images were captured by confocal microscopy (a Leica SP5 confocal microscope). All images were processed in Adobe Photoshop.

2.5. Statistics

Statistical analyses were carried out with GraphPad Prism 6 software using either the unpaired Student's t-test or One-way ANOVA, and all quantitative data are shown as mean ± SEM. No statistical method was used to predetermine sample size. No samples were excluded. The experiments were not randomized. The investigators were not blinded to allocation during the experiments and outcome assessment.

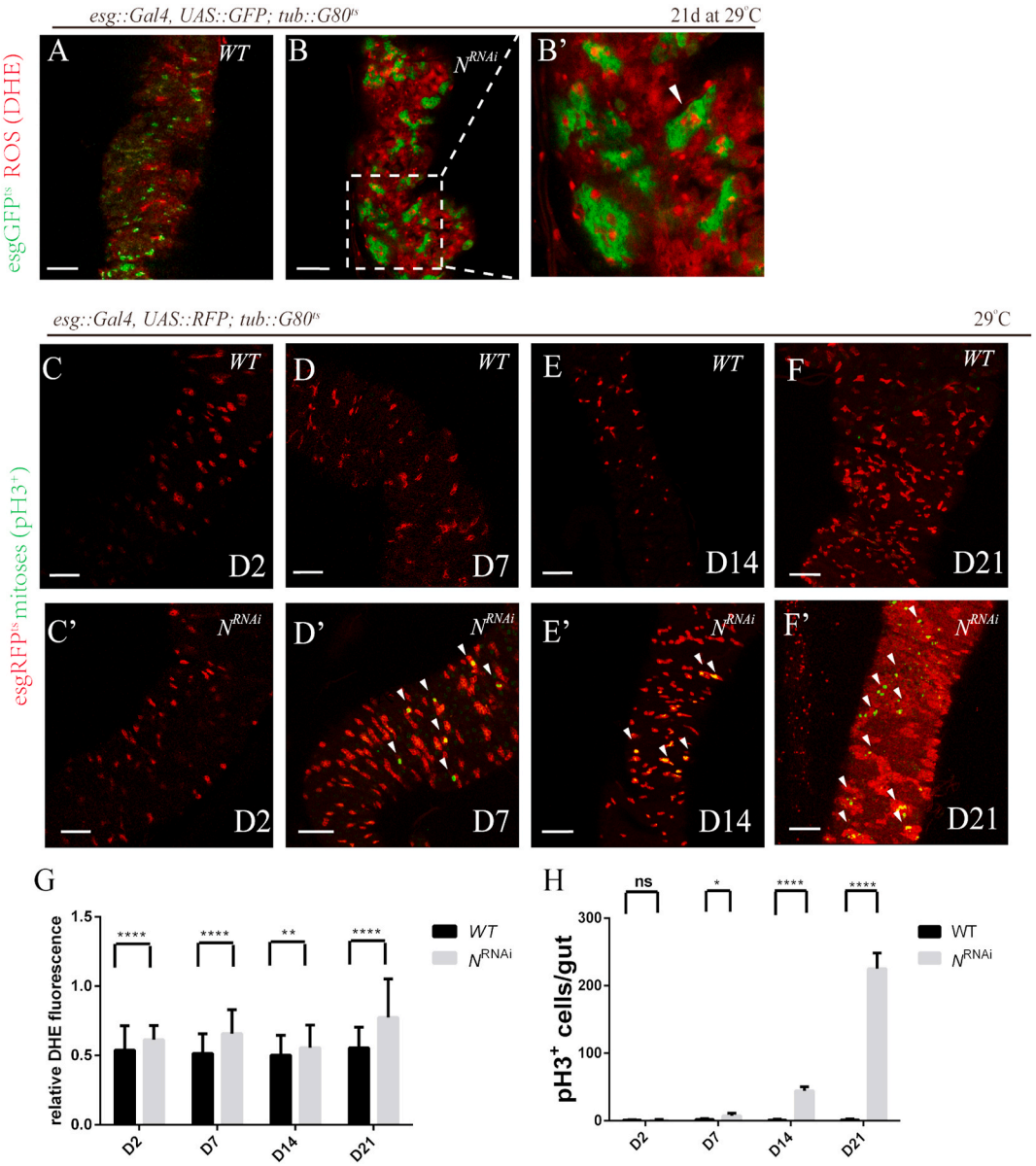

Fig. 3. *Notch* knockdown increased intracellular ROS and induced hyperproliferation.
(A) DHE fluorescence in intestines from flies expressing GFP only (control, "WT") under the control of *esg-Gal4* via the TAEGET system. Transgenes was induced by shifting flies to restrictive temperature (29 °C). Intestines were analyzed 21 days after induction. Scale bars, 50 μm. (B) Depletion of *N* resulted in tumor-like pathological phenotype. DHE fluorescence in intestines from flies expressing N^{RNAi} and GFP ("N^{RNAi}") via the TAEGET system at 29 °C for 21 days. (B′) Higher magnification of the boxed area of (B). High levels of ROS were detected in esg$^+$ cells (arrowhead points out one example). (C–F) Increased proliferative capacity of ISCs in N^{RNAi} flies versus control. pH3 staining (in green) of intestines from flies expressing RFP only (Control, "WT") (C–F) and N^{RNAi} and RFP ("N^{RNAi}") (C′–F′) under the control of *esg-Gal4* via the TAEGET system. Transgenes were induced by shifting flies to restrictive temperature (29 °C). Representative images of intestines at 29 °C for 2, 7, 14 and 21 days are shown. White arrowheads: mitotic (anti-Phosphohistone H3/PH3 positive) cells. Scale bars, 50 μm. (G) Increase in ROS levels of N^{RNAi} flies compared with control. Quantification of relative DHE fluorescence in intestines from flies expressing N^{RNAi} and GFP ("N^{RNAi}") and GFP only (control, "WT") at 29 °C for 2, 7, 14 and 21 days are shown (average and SEM; Student's *t*-test and and Mann-Whitney test). Relative DHE fluorescence in ISCs is normalized to DHE fluorescence in adjacent ECs. (H) Higher proliferation rates of N^{RNAi} flies compared with control. Amounts of pH3$^+$ cells in intestines from flies expressing N^{RNAi} and GFP ("N^{RNAi}") and GFP only (control, "WT") at 29 °C for 2, 7, 14 and 21 days is shown in the histogram (average and SEM; Student's *t*-test and Mann-Whitney test). (For interpretation of the references to colour in this figure legend, the reader is referred to the Web version of this article.)

3. Results

3.1. The ROS levels of ISCs remained low and increase with ageing

The binary system *escargot-Gal4* [*esg-Gal4*]-driven GFP was used to mark ISCs and EBs with GFP [34] (Fig. 1A-A'; Fig. 1B). To quantify the ROS levels in ISCs, we measured the intracellular ROS levels *in vivo* using dihydroethidium (DHE), a redox-sensitive dye that exhibits increased fluorescence intensity when oxidized (Owusu-Ansh et al., 2008). Cells in the ISCs had significantly lower ROS than their neighboring differentiated ECs (Fig. 1A'', D). Similarly, we found lower superoxide levels in the ISCs using MitoSox red staining (Fig. 1B'), a unique fluorogenic dye that allows for selective detection of superoxide production in the mitochondria [35]. Nrf2/CncC is a major regulator of the cellular redox state (Hochmuth et al., 2011). To test whether the low levels of ROS in the ISCs is regulated by the Nrf2/CncC, we assessed GFP reporter based on the upstream regulatory sequences of the CncC target gene *gstD1* (*gstD1*::*GFP*) in the posterior midgut. We observed that *gstD1*::*GFP* was

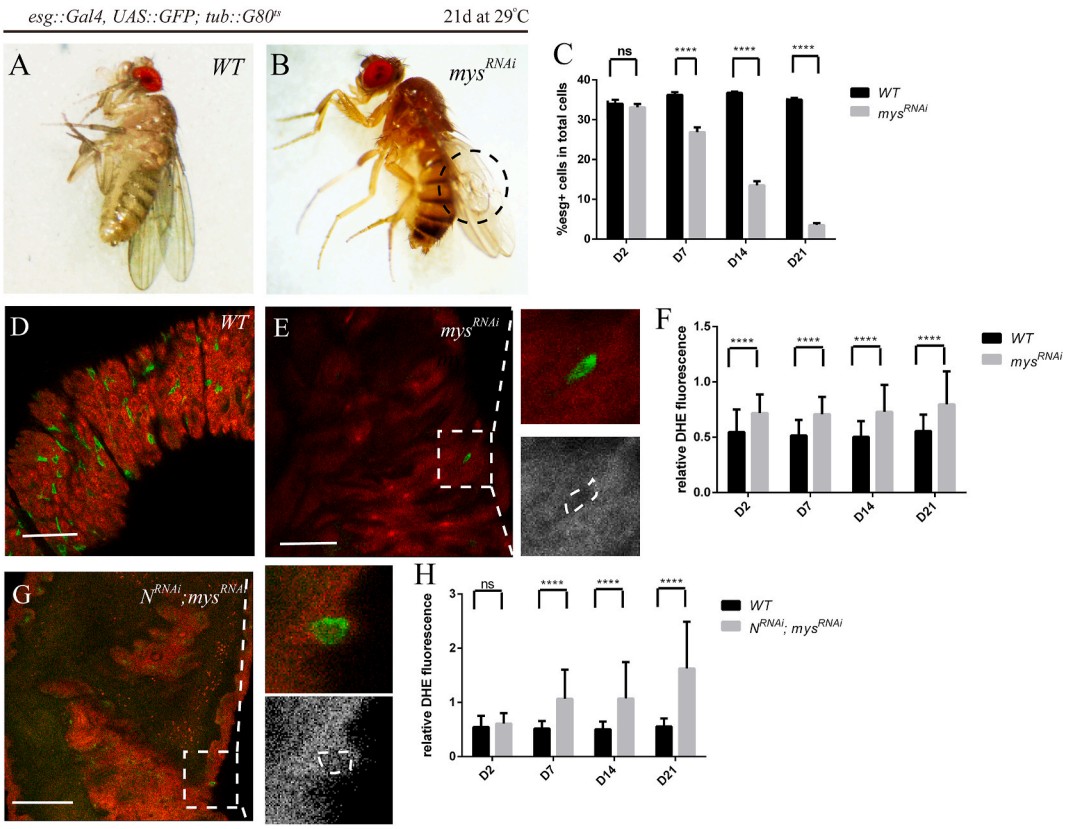

Fig. 4. *mys* RNAi-mediated loss of ISCs accompanied by increased ROS levels

(A, B) Blistering phenotype of wings in mys^{RNAi} flies. Representative wings from flies expressing GFP only (control, "*WT*") (A) and mys^{RNAi} (B) under the control of *esg-Gal4* via the TAEGET system. Transgenes was induced by shifting flies to restrictive temperature (29 °C). Wings were observed 21 days after induction. Note that the flies of mys^{RNAi} had characteristic wing blistering phenotype indicated by dotted line. (C) Significant decrease in number of ISCs in mys^{RNAi} flies compared with control. Quantifications of the percentage of *esg-GFP*$^+$ cells in intestines from flies expressing mys^{RNAi} and GFP ("mys^{RNAi}") and GFP only (control, "*WT*") at 29 °C for 2, 7, 14 and 21 days are shown (average and SEM; Student's *t*-test and Mann-Whitney test.). (D) DHE fluorescence in intestines from flies expressing only GFP (control, "*WT*") under the control of *esg-Gal4* via the TAEGET system. Transgenes was induced by shifting flies to restrictive temperature (29 °C). Intestines were analyzed 21 days after induction. Scale bars, 50 μm. (E) Representative image of ISCs loss phenotype in ECM-deprived model (mys^{RNAi}). DHE fluorescence in intestines from flies expressing mys^{RNAi} and GFP (mys^{RNAi}) under the control of *esg-Gal4* via the TAEGET system. Transgenes was induced by shifting flies to restrictive temperature (29 °C). Intestines were analyzed 21 days after induction. Note that the *esg-GFP*$^+$ cells are very scarce. Higher magnification of the boxed area of (E) are shown in the right panels. DHE staining is shown separately in the lower panel. Scale bars, 50 μm. (F) Increase in ROS levels of surviving ISCs in mys^{RNAi} flies compared with control. Quantifications of relative DHE fluorescence in intestines from flies expressing mys^{RNAi} and GFP ("mys^{RNAi}") and only GFP (control, "*WT*") at 29 °C for 2, 7, 14 and 21 days are shown (average and SEM; Student's *t*-test and Mann-Whitney test). Relative DHE fluorescence in ISCs was normalized to DHE fluorescence in adjacent ECs. (G) Representative image of ISCs loss phenotype in ECM-deprived tumor model (N^{RNAi}; mys^{RNAi}). DHE fluorescence in intestines from flies expressing N^{RNAi}, mys^{RNAi} and GFP (N^{RNAi}; mys^{RNAi}) under the control of *esg-Gal4* via the TAEGET system. Transgenes was induced by shifting flies to restrictive temperature (29 °C). Intestines were analyzed 21 days after induction. Higher magnification of the boxed area of (G) are shown in the right panels. DHE staining is shown separately in the lower panel. Scale bars, 50 μm. (H) Significant increase in ROS levels of ISCs in *N*- and *mys*-depleted flies compared with control. Quantifications of relative DHE fluorescence in intestines from flies expressing N^{RNAi}, mys^{RNAi} and GFP (N^{RNAi}; mys^{RNAi}) and GFP only (control, "*WT*") at 29 °C for 2, 7, 14 and 21 days are shown (average and SEM; Student's *t*-test and Mann-Whitney test). Relative DHE fluorescence in ISCs was normalized to DHE fluorescence in adjacent ECs.

expressed highly in ISCs (Fig. 1C-C″). CncC thus appeared to be required in ISCs to maintain low levels of ROS. Previous studies observed age-associated elevated ROS levels and loss of epithelial homeostasis in wild-type flies, where ISCs progressively over-proliferated in aging animals [36]. We examined ISC proliferation rates in the intestinal epithelium by assessing the frequency of phosphorylated histone H3-positive (pH3$^+$) cells. Indeed, the ROS levels and proliferation rates of ISCs at Day 21 adult flies were higher than those at Day 7 (Fig. 1D and E), implicating that the degeneration of the intestinal epithelium was intensified with ageing.

3.2. Perturbation of ROS levels in ISCs barely disrupted the intrinsic homeostasis under physiological condition

As a low intracellular concentration of ROS has been proposed critical for stemness and pluripotency of stem cells [1], we tested whether changes of ROS affected the ISCs homeostasis. We utilized the Temporal and Regional Gene Expression Targeting (TARGET) system to spatially and temporally regulate the level of ROS in ISCs (and EBs) [37]. We overexpressed ROS-scavenging enzymes through expression of a *UAS-CncC* transgene [38], a *UAS-Catalase* transgene or a *UAS-Sod2* transgene [39], specifically in the *esg*$^+$ cells, and found no reduction of ROS levels in *esg*$^+$ cells (Fig. 2A). These data suggested that the ROS levels of ISCs under physiological condition were probably very low that further reduction might be difficult. Meanwhile, ISCs number and overall phenotype resembled wild-types (Fig. 2C). In parallel, when CncC, Catalase and Sod2 were knocked down via a $UAS\text{-}CncC^{RNAi}$ transgene [38], a $UAS\text{-}Catalase^{RNAi}$ transgene [40], or a $UAS\text{-}Sod2^{RNAi}$ transgene [40], ROS levels in ISCs could be significantly upregulated (Fig. 2B). However, ISCs number and overall phenotype still resembled those of wild-types (Fig. 2C), implicating an intrinsic homeostatic range of ROS in ISCs.

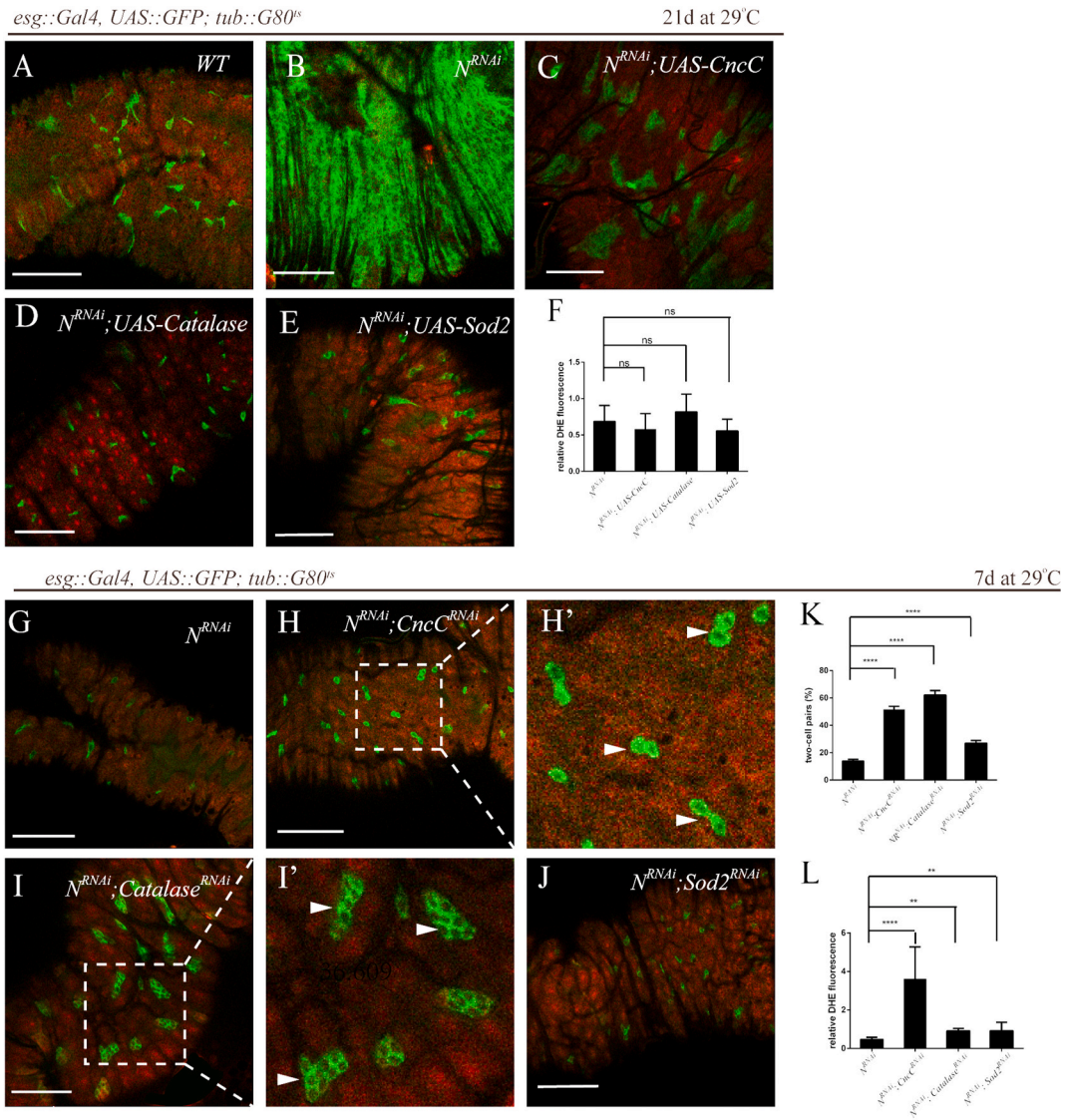

Fig. 5. Differential ISC redox levels modified *Notch*^{RNAi}-mediated ISC-like tumor phenotype

(A–F) Overexpression of ROS-scavenging enzymes suppressed ISC over-proliferation in the N^{RNAi} context. DHE fluorescence in intestines from flies expressing GFP only (Control, "*WT*") (A), N^{RNAi} and GFP (N^{RNAi}) (B), N^{RNAi}, CncC and GFP (N^{RNAi}; *UAS-CncC*) (C), N^{RNAi}, Catalase and GFP (N^{RNAi}; *UAS-Catalase*) (D) and N^{RNAi}, Sod2 and GFP (N^{RNAi}; *UAS-Sod2*) (E) under the control of *esg*::*Gal4* via the TAEGET system. No significant reduction in ROS levels with over-expression of ROS-scavenging enzymes at the late stage of tumor induction by N^{RNAi} and quantifications are shown in (F) (average and SEM; ANOVA test). Relative DHE fluorescence in ISCs was normalized to DHE fluorescence in adjacent ECs. Transgenes was induced by shifting flies to restrictive temperature (29 °C). Intestines were analyzed 21 days after induction. Representative confocal images are shown. Scale bars, 50 μm. (G–L) An increase of doublets or clusters of ISCs upon silencing ROS-scavenging enzymes in the N^{RNAi} context at the early stage of tumor induction. DHE fluorescence in intestines from flies expressing N^{RNAi} and GFP (N^{RNAi}) (G), N^{RNAi}, CncC^{RNAi} and GFP (N^{RNAi}; *CncC*^{RNAi}) (H), N^{RNAi}, Catalase^{RNAi} and GFP (N^{RNAi}; *Catalase*^{RNAi}) (I) and N^{RNAi}, Sod2^{RANi} and GFP (N^{RNAi}; *Sod2*^{RNAi}) (J) under the control of *esg-Gal4* via the TAEGET system. Transgenes was induced by shifting flies to restrictive temperature (29 °C). Intestines were analyzed 7 days after induction. (H′) Higher magnification of the boxed area of (H). Two-cell pairs are indicated (arrowheads). (I′) Higher magnification of the boxed area of (I). Small tumor-like clusters are also indicated (arrowheads). Quantifications are shown in (K) (average and SEM; ANOVA test). Further elevation of ROS levels upon silencing ROS-scavenging enzymes in the N^{RNAi} context. Quantifications of relative DHE fluorescence are shown in (L) (average and SEM; ANOVA test). Relative DHE fluorescence in ISCs was normalized to DHE fluorescence in adjacent ECs. Representative confocal images are shown. Scale bars, 50 μm.

3.3. Depletion of notch resulted in ISC-like tumor model and elevated ROS levels

ROS have been recently proposed to be involved in tumor progression. Previous studies revealed that cancer cells often exhibit increased generation of ROS compared with normal cells [11]. To test the role of redox regulation in tumor development, we firstly constructed a tumor-like pathological model caused by the depletion of *N*. When *N-RNAi* [41] was induced in ISCs under the control of *esg-Gal4*, all intestines were able to develop into tumor-like phenotype (Fig. 3A, B-B′). In line with previous reports, the intracellular ROS levels in tumor-like ISCs increased significantly (Fig. 3G), which was accompanied by a gradual increase in proliferation rates (Fig. 3C–F', H), suggesting that increased ROS stress in cancer cells may in turn further contribute to hyperproliferation of ISCs and tumor formation.

3.4. Depletion of β-integrin resulted in ISC loss phenotype and elevated ROS levels

Tumor cells are usually displaced from their matrix niches in the early stages of metastasis. The data described above suggested that high level of ROS was essential in ISCs over-proliferation in the N^{RNAi} ISC

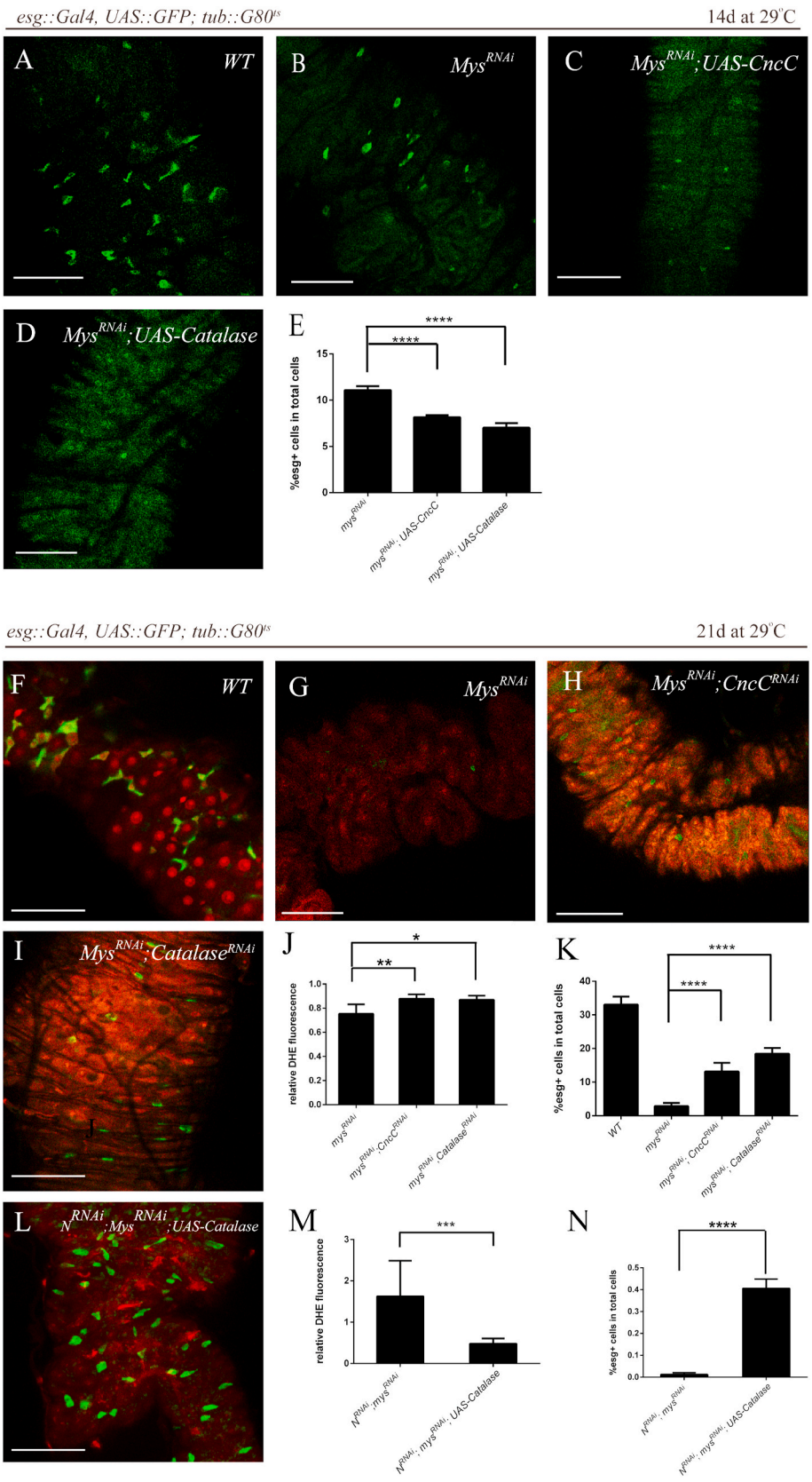

Fig. 6. Differential ISC redox levels modified Mys^{RNAi}-mediated ISC loss phenotype

(A–E) More severe ISCs loss phenotype upon overexpressing ROS-scavenging enzymes in the *mys*^{RNAi} context. Intestines from flies expressing only GFP (control, "*WT*") (A), *mys*^{RNAi} and GFP (*mys*^{RNAi}) (B), *mys*^{RNAi}, CncC and GFP (*mys*^{RNAi}; *UAS-CncC*) (C) and *mys*^{RNAi}, Catalase and GFP (*mys*^{RNAi}; *UAS-Catalase*) (D) under the control of *esg-Gal4* via the TAEGET system. Transgenes was induced by shifting flies to restrictive temperature (29 °C). Intestines were analyzed 14 days after induction. Representative confocal images are shown. Scale bars, 50 μm. Quantifications of the percentage of *esg* > *GFP*$^{+}$ cells in intestines are shown in (E). (average and SEM; ANOVA test). (F–K) Rescue of ISCs loss phenotype upon depleting ROS-scavenging enzymes in the *mys*^{RNAi} context. DHE fluorescence in intestines from flies expressing only GFP (control, "*WT*") (F), *mys*^{RNAi} and GFP (*mys*^{RNAi}) (G), *mys*^{RNAi}, CncC^{RNAi} and GFP (*mys*^{RNAi}; *CncC*^{RNAi}) (H) and *mys*^{RNAi}, Catalase^{RNAi} and GFP (*mys*^{RNAi}; *Catalase*^{RNAi}) (I) under the control of *esg-Gal4* via the TAEGET system. Transgenes were induced by shifting flies to restrictive temperature (29 °C). Intestines were analyzed 21 days after induction. Representative images are shown. Scale bars, 50 μm. Elevated ROS levels upon depleting ROS-scavenging enzymes in the *mys*^{RNAi} context and quantifications of relative DHE fluorescence are shown (J) (average and SEM; ANOVA test). Relative DHE fluorescence in ISCs is normalized to DHE fluorescence in adjacent ECs. Quantifications of the percentage of *esg* > *GFP*$^{+}$ cells in intestines are shown in (K) (average and SEM; ANOVA test). (L–N) Rescue of ISCs loss phenotype upon expressing Catalase in the *N*- and *mys*-depleted context. Transgenes were induced by shifting flies to restrictive temperature (29 °C). Intestines were analyzed 21 days after induction. Representative confocal images are shown (L). Scale bars, 50 μm. Decrease in ROS levels of ISCs upon overexpressing Catalase in the *N*- and *mys*-depleted context and quantifications of relative DHE fluorescence are shown in (M) (average and SEM; Student's *t*-test). Relative DHE fluorescence in ISCs was normalized to DHE fluorescence in adjacent ECs. Significant increase in number of ISCs upon overexpressing Catalase in the *N*- and *mys*-depleted context. Quantifications of the percentage of *esg* > *GFP*$^{+}$ cells are shown in (N) (average and SEM; Student's *t*-test and Mann-Whitney test).

tumors. We then examined whether it was similar in metastasis stages. Attachment to extracellular matrix (ECM) is required for the survival and proliferation of normal epithelial cells. Epithelial tumor cells, however, often acquire "anchorage independence", a property that may contribute to their ability to invade and grow in foreign environments. We first examined the role of matrix attachment of ISCs. Previous studies have shown integrin-mediated cell adhesion is required for ISC maintenance [42]. We utilized the TARGET system to deplete *mys* in ISCs to form matrix-deprived model. Having confirmed the functionality of the RNAi lines by the characteristic wing blistering phenotype observed upon *mys* depletion (Brower and Jaffe, 1989) (Fig. 4A and B), we found that depletion of *mys* subunit resulted in loss of ISCs in normal fly from Day7 after shift to the restrictive temperature (Fig. 4C–E). To assay the redox state in ISCs that are still alive, we monitored endogenous ROS levels *in vivo* by using DHE. Interestingly, ROS levels increased moderately in ISCs, similar to that in N^{RNAi} ISC tumors (Fig. 5F). Next, we utilized the TARGET system to deplete both *N* and *mys* in ISCs to establish the matrix-deprived tumor model, wherein metastatic tumor initiating cells were mimicked. A severe ISC loss phenotype was observed (Fig. 4G) and the ROS levels of the surviving *N*- and *mys*-depleted ISCs increased remarkably (Fig. 4H).

3.5. ROS manipulations modified N^{RNAi} ISC-like tumors

As we observed similar moderately elevated ROS levels in both tumor-like ISCs (N^{RNAi}) and extracellular matrix (ECM)-deprived ISCs (mys^{RNAi}), we wondered whether there was difference underneath the similarity. When CncC, Catalase or SOD2 was overexpressed in the N^{RNAi} context, tumor formation was significantly prevented (Fig. 5A–E) albeit the ROS levels were not decreased at the late stage of tumor formation (Fig. 5F). On the other hand, when ROS levels were elevated (Figure 5L) upon silencing of CncC, Catalase or SOD2 in the N^{RNAi} context, we observed an increase of doublets of ISCs in the case of $CncC^{RNAi}$ or $SOD2^{RNAi}$ (Fig. 5 G-H′, J, K) and even small tumor-like clusters in the case of Catalase ^{RNAi} in the early tumor induction stage (Fig. 5I-I'). Taken together, these results suggested that the increased ROS aggravated hyperproliferation of ISCs and tumor formation in N^{RNAi} tumors, implicating a tumor-promoting role of ROS in such context.

3.6. Differential ISC redox levels modified Mys^{RNAi}-mediated ISC loss phenotype

To explore the possibility that moderately high level of ROS caused by mys^{RNAi} was the cause of ISCs loss, we reduced ROS levels upon expressing of CncC and Catalase in the mys^{RNAi} fly. Surprisingly, we found that downregulation of ROS levels aggravated the loss phenotype of ISCs (Fig. 6A–E). In contrast, upregulation of ROS levels (Fig. 6J) partially suppressed the ISCs loss (Fig. 6F–I, K). Collectively, these results suggested that ROS has a pro-surviving capacity in the ECM-deprived ISCs.

However, reducing ROS (Figure 6M) in the ECM-deprived N^{RNAi} ISCs prevented ISCs loss (Figure 6L, N), which was opposite to those simple ECM-deprived ISCs, suggesting that excessive amounts of ROS could be toxic to the cells and antioxidants might promote the survival of tumor-initiating cells that lack extracellular attachment. These results indicated an unanticipated mechanism for tumor cell survival in altered matrix environments through antioxidants.

4. Discussion

Tissue homeostasis is regulated by tightly controlled division and differentiation of multipotent somatic stem cells that give rise to different cell types of a given tissue. These processes need a precisely regulated ROS levels. In our work, we found that ISCs maintain low intracellular ROS levels and prevent excessive proliferation in normal intestine. Neither upregulation nor downregulation of ROS levels significantly affected ISCs, implicating that the self-renewal of ISCs in young flies could maintain in a homeostatic state. However, old intestinal epithelia exhibit significantly elevated ROS levels in ISCs, which is related to age-related increase in ISC proliferation rates and disruption of epithelial homeostasis.

Mounting evidence suggests that many types of cancer cell have increased levels of ROS [43]. Tumor suppressor and oncogenic pathways frequently mutated in cancer commonly result in increased accumulation of ROS [44–47]. An increase in ROS is associated with abnormal cancer cell growth and reflects a disruption of redox homeostasis. The *Notch* signaling pathway regulates cell fate determination during development and alterations of the *Notch* signaling can lead to a variety of disorders including human malignancies. In this work, depletion of *N* could induce an ISCs-like tumor phenotype, which facilitated us to study the role of ROS in tumor. We observed that increased oxidation of ISCs in *N-RNAi* conditions was accompanied by elevated proliferation rates, and we further found that tumor formation could be obviously prevented when we reduce ROS levels in ISCs-like tumor cells through overexpression of oxidant scavenger proteins. Our work suggested that increased ROS stress in cancer cells may contribute to hyperproliferation of tumor initiating cells and tumor formation, which raises the possibility that regulation of ROS could be a potential therapy for *Notch*-related cancer [48]. Furthermore, we observed that there was no tumor formation throughout our experiment when we downregulated the fatty acid oxidation (FAO) pathway in *N-RNAi* conditions (data not shown), which was in line with a previous report that cancer cells deprived of glucose maintain ATP production through FAO [49].

Normal epithelial cells require matrix attachment for survival and the ability of tumor cells to survive outside their natural extracellular matrix (ECM) niches during metastasis is dependent on acquisition of anchorage independence [50]. What roles ROS plays in this progress remains elusive. To address this question, we genetically knockdown *mys* in ISCs to mimic a ECM-deprived model, and we found ISCs number declined dramatically. This is consistent with previous work [51]. Unexpectedly, downregulation of ROS levels aggravated ISCs loss phenotype, and the survived mys^{RNAi} ISCs all had elevated levels of ROS. Previous studies revealed that detachment of epithelial cells from ECM causes an ATP deficiency due to loss of glucose transport [51]. Indeed, we also found that ISCs loss phenotype could be rescued after feeding the *mys-RNAi* flies high-glucose food (data not shown). More evidence is needed to confirmed whether the loss of ISC was caused by ATP deficiency. Overall, our results suggest that moderate elevation of ROS in ECM-deprivation model is not the main cause of ISCs loss but a stress response during detachment from ECM. Previous studies also revealed that increase ROS would be correlated with anoikis protection of endothelial cells during cell detachment from ECM [52,53]. Taken together, we speculate that ROS is a key signaling molecules eliciting pro-survival signals protection from ISCs anoikis in the absence of ECM contact.

Increased ROS levels are considered to be closely linked to the accelerated formation of metastasis, and the removal of ROS is a rational strategy to inhibit metastasis. However, there are also controversial results reported thus far, and ROS should have diverse effects on tumor metastasis [21]. Through depletion of *N* and *mys* in ISCs, which resembled metastatic tumor cells, we observed severe ISCs loss symptoms. A previous study in the fly midgut also found that reducing integrins in N^- or Apc^- tumor cells inhibited their growth, and demonstrated that tumor cells competed with ECs for attachment to the basement membrane, via integrine-mediated adhesion [25]. It is noteworthy that high levels of ROS in N^- mys^- tumor cells (higher than N^{RNAi} or mys^{RNAi} alone) were observed in our research. Consistently, matrix detachment associated with tumorigenesis lead to excess production of ROS [54–58], which can damage cellular components and compromise cell viability [59]. Collectively, we hypothesize that excessive accumulation of ROS, beyond the cellular tolerant threshold, is the main cause of ISCs loss phenotype in ECM-deprived tumor model. This

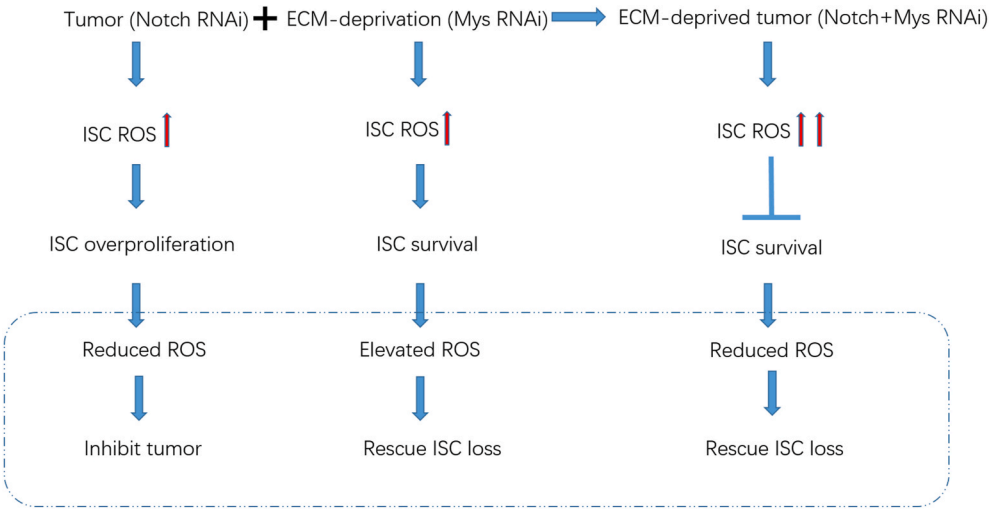

Fig. 7. Summary of the levels and regulations of ROS in ISCs under different conditions

N depletion induced a moderate increase of intrinsic ROS generation (red arrow), leading to a hyperproliferation of ISCs and tumor formation. Downregulation of ROS in tumor cells could suppressed the hyperproliferation phenotype. ECM-deprivation caused by *mys* depletion could lead to ISCs loss phenotype, also induced a moderate intrinsic increase of ROS generation (red arrow). Further increased ROS in turn facilitated the survival of ECM-deprived ISCs while reduced ROS exacerbated the loss of ECM-deprived ISCs. *N*- and *mys*-depleted ISCs, which resembled metastatic tumor cells, harbored even higher ROS levels that were toxic (two red arrows) and were subjected to more severe oxidative stress, which could be partially prevented by ectopic supply of antioxidant enzymes. (For interpretation of the references to colour in this figure legend, the reader is referred to the Web version of this article.)

interpretation is supported by the fact that antioxidants can rescue ISCs loss phenotype in ECM-deprived tumor model. Collectively, these results suggested that antioxidant scavenges excessive ROS and may promote the survival of tumor cells in pathological matrix environments and thus enhance malignancy.

Taken together, our results revealed the intracellular redox level is a critical cell fate determinant of stem cells and tumor cells under various conditions and suggested that the antioxidant-based intervention of stem cells and tumors should be formulated with caution according to the specific situations (Fig. 7).

Acknowledgments

We thank Drs. Ohlstein and Perrimon for sharing key fly strains, Wei Wu at Core Facility of *Drosophila* Resource and Technology, SIBCB, CAS for providing fly service and fly stocks, the Tsinghua *Drosophila* Resource Center for providing fly stocks. This study was financially supported by the Natural Science Foundation of Fujian Province, China (No. 2018J01733) and the National Natural Science Foundation of China (#31070877).

References

[1] K. Ito, et al., Regulation of oxidative stress by ATM is required for self-renewal of haematopoietic stem cells, Nature 431 (2004) 997–1002.
[2] J. Liu, et al., Bmi1 regulates mitochondrial function and the DNA damage response pathway, Nature 459 (2009) 387–392.
[3] E. Owusu-Ansah, U. Banerjee, Reactive oxygen species prime Drosophila haematopoietic progenitors for differentiation, Nature 461 (2009) 537–541.
[4] J. Smith, E. Ladi, M. Mayer-Proschel, M. Noble, Redox state is a central modulator of the balance between self-renewal and differentiation in a dividing glial precursor cell, Proc. Natl. Acad. Sci. U. S. A. 97 (2000) 10032–10037.
[5] Z. Tothova, D.G. Gilliland, FoxO transcription factors and stem cell homeostasis: insights from the hematopoietic system, Cell Stem Cell 1 (2007) 140–152.
[6] M. Tsatmali, E.C. Walcott, K.L. Crossin, Newborn neurons acquire high levels of reactive oxygen species and increased mitochondrial proteins upon differentiation from progenitors, Brain Res. 1040 (2005) 137–150.
[7] J. Boonstra, J. Post, Molecular events associated with reactive oxygen species and cell cycle progression in mammalian cells, Gene 337 (2004) 1–13.
[8] F.Q. Schafer, G.R. Buettner, Redox environment of the cell as viewed through the redox state of the glutathione disulfide/glutathione couple, Free Radical Biol. Med. 30 (2001) 1191–1212.
[9] M.K. Paul, B. Bharti, D.O. Darmawan, C. Richard, V.L. Ha, W.D. Wallace, A. T. Chon, A.E. Hegab, G. Tristan, D.A. Elashoff, Dynamic changes in intracellular ROS levels regulate airway basal stem cell homeostasis through Nrf2-dependent Notch signaling, Cell Stem Cell 15 (2014) 199–214.
[10] G. Perry, A.K. Raina, A. Nunomura, T. Wataya, L.M. Sayre, M.A. Smith, How important is oxidative damage? Lessons from Alzheimer's disease, Free Radical Biol. Med. 28 (2000) 831–834.
[11] T.P. Szatrowski, C.F. Nathan, Production of large amounts of hydrogen peroxide by human tumor cells, Canc. Res. 51 (1991) 794–798.
[12] S. Kawanishi, Y. Hiraku, S. Pinlaor, N. Ma, Oxidative and nitrative DNA damage in animals and patients with inflammatory diseases in relation to inflammation-related carcinogenesis, Biol. Chem. 387 (2006) 365–372.
[13] S. Toyokuni, K. Okamoto, J. Yodoi, H. Hiai, Persistent oxidative stress in cancer, FEBS Lett. 358 (1995) 1–3.
[14] S. Elchuri, T.D. Oberley, W. Qi, R.S. Eisenstein, L. Jackson Roberts, H. Van Remmen, C.J. Epstein, T.T. Huang, CuZnSOD deficiency leads to persistent and widespread oxidative damage and hepatocarcinogenesis later in life, Oncogene 24 (2005) 367–380.
[15] Y.P. Lu, Y.R. Lou, P. Yen, H.L. Newmark, O.I. Mirochnitchenko, M. Inouye, M. T. Huang, Enhanced skin carcinogenesis in transgenic mice with high expression of glutathione peroxidase or both glutathione peroxidase and superoxide dismutase, Canc. Res. 57 (1997) 1468–1474.
[16] R.A. Egler, E. Fernandes, K. Rothermund, S. Sereika, N. De Souza-Pinto, P. Jaruga, M. Dizdaroglu, E.V. Prochownik, Regulation of reactive oxygen species, DNA damage, and c-Myc function by peroxiredoxin 1, Oncogene 24 (2005) 8038–8050.
[17] J.P. Fruehauf, J.R. Meyskens FL, Reactive oxygen species: a breath of life or death? Clin. Canc. Res. : Off. J. Am. Assoc. Canc. Res. 13 (2007) 789–794.
[18] E. Kadosh, et al., The gut microbiome switches mutant p53 from tumour-suppressive to oncogenic, Nature 586 (2020) 133–138, https://doi.org/10.1038/s41586-020-2541-0.
[19] S. Prasad, S.C. Gupta, A.K. Tyagi, Reactive oxygen species (ROS) and cancer: role of antioxidative nutraceuticals, Canc. Lett. 387 (2017) 95–105.
[20] W.S. Wu, The signaling mechanism of ROS in tumor progression, Canc. Metastasis Rev. 25 (2006) 695–705.
[21] M. Nishikawa, Reactive oxygen species in tumor metastasis, Canc. Lett. 266 (2008) 53–59.
[22] A. Ayyaz, H. Jasper, Intestinal inflammation and stem cell homeostasis in aging Drosophila melanogaster, Front. Cell. Infect. Microbiol. 3 (2013) 98.
[23] B. Lemaitre, I. Miguel-Aliaga, The digestive tract of Drosophila melanogaster, Annu. Rev. Genet. 47 (2013) 377–404.
[24] H. Jiang, B.A. Edgar, Intestinal stem cell function in Drosophila and mice, Curr. Opin. Genet. Dev. 22 (2012) 354–360.
[25] P.H. Patel, D. Dutta, B.A. Edgar, Niche appropriation by Drosophila intestinal stem cell tumours, Nat. Cell Biol. 17 (2015) 1182–1192.
[26] Y. Apidianakis, L.G. Rahme, Drosophila melanogaster as a model for human intestinal infection and pathology, Dis. Models Mech. 4 (2011) 21–30.
[27] P. Bergman, S. Seyedoleslami Esfahani, Y. Engstrom, Drosophila as a model for human diseases-focus on innate immunity in barrier epithelia, Curr. Top. Dev. Biol. 121 (2016) 29–81.
[28] C.A. Micchelli, P. Norbert, Evidence that stem cells reside in the adult Drosophila midgut epithelium, Nature 439 (2006) 475–479.
[29] O. Benjamin, S. Allan, The adult Drosophila posterior midgut is maintained by pluripotent stem cells, Nature 439 (2006) 470–474.
[30] A. Amcheslavsky, J. Jiang, I.P. Yt, Tissue damage-induced intestinal stem cell division in Drosophila, Cell Stem Cell 4 (2009) 49–61.
[31] P.H. Patel, D. Dutta, B.A. Edgar, Niche appropriation by Drosophila intestinal stem cell tumours。, Nat. Cell Biol. 17 (2015) 1182–1192.
[32] B. Ohlstein, A. Spradling, The adult Drosophila posterior midgut is maintained by pluripotent stem cells, Nature 439 (2006) 470–474.
[33] H. Hamidi, J. Ivaska, Every Step of the Way: Integrins in Cancer Progression and Metastasis, vol. 18, 2018, pp. 533–548.

[34] A.H. Brand, N. Perrimon, Targeted Gene Expression as a Means of Altering Cell Fates and Generating Dominant Phenotypes, vol. 118, Development, Cambridge, England, 1993, pp. 401–415.
[35] F. Scialo, A. Sriram, R. Stefanatos, R.V. Spriggs, S.H.Y. Loh, L.M. Martins, A. Sanz, Mitochondrial complex I derived ROS regulate stress adaptation in Drosophila melanogaster, Redox Biol. 32 (2020) 101450.
[36] Hochmuth CE, Biteau B, Bohmann D and Jasper H. Redox regulation by Keap1 and Nrf2 controls intestinal stem cell proliferation in Drosophila. Cell Stem Cell 8: 188-199.
[37] S.E. Mcguire, P.T. Le, A.J. Osborn, K. Matsumoto, R.L. Davis, Spatiotemporal rescue of memory dysfunction in Drosophila, Science 302 (2003) 1765–1768. New York, NY.
[38] G.P. Sykiotis, D. Bohmann, Keap1/Nrf2 signaling regulates oxidative stress tolerance and lifespan in Drosophila, Dev. Cell 14 (2008) 76–85.
[39] A. Hussain, A. Pooryasin, Inhibition of Oxidative Stress in Cholinergic Projection Neurons Fully Rescues Aging-Associated Olfactory Circuit Degeneration in Drosophila, vol. 7, 2018.
[40] L.A. Perkins, et al., The transgenic RNAi project at Harvard medical school: resources and validation, Genetics 201 (2015) 843–852.
[41] B.E. Housden, A. Terriente-Felix, S.J. Bray, Context-dependent enhancer selection confers alternate modes of notch regulation on argos, Mol. Cell Biol. 34 (2014) 664–672.
[42] Lin G, Zhang X, Ren J, Pang Z, Wang C, Xu N and Xi R. Integrin signaling is required for maintenance and proliferation of intestinal stem cells in Drosophila. Dev. Biol. 377: 177-187.
[43] H. kim, et al., Sulfiredoxin inhibitor induces preferential death of cancer cells through reactive oxygen species-mediated mitochondrial damage, Free Radical Biol. Med. 91 (2016) 264–274.
[44] O. Vafa, M. Wade, S. Kern, M. Beeche, T.K. Pandita, G.M. Hampton, G.M. Wahl, c-Myc can induce DNA damage, increase reactive oxygen species, and mitigate p53 function: a mechanism for oncogene-induced genetic instability, Mol. Cell 9 (2002), 0-1044.
[45] V. Nogueira, Y. Park, C.C. Chen, P.Z. Xu, M.L. Chen, I. Tonic, T. Unterman, N. Hay, Akt determines replicative senescence and oxidative or oncogenic premature senescence and sensitizes cells to oxidative apoptosis, Canc. Cell 14 (2008) 458–470.
[46] A.A. Sablina, A.V. Budanov, G.V. Ilyinskaya, L.S. Agapova, J.E. Kravchenko, P. M. Chumakov, The antioxidant function of the p53 tumor suppressor, Nat. Med. 11 (2005) 1306–1313.
[47] K. Bensaad, E.C. Cheung, K.H. Vousden, Modulation of intracellular ROS levels by TIGAR controls autophagy, EMBO J. 28 (2009) 3015–3026.
[48] V. Slaninova, M. Krafcikova, R. Perez-Gomez, P. Steffal, L. Trantirek, S.J. Bray, A. Krejci, Notch Stimulates Growth by Direct Regulation of Genes Involved in the Control of Glycolysis and the Tricarboxylic Acid Cycle, vol. 6, 2016, p. 150155.
[49] M. Buzzai, D.E. Bauer, R.G. Jones, R.J. Deberardinis, G. Hatzivassiliou, R. L. Elstrom, C.B. Thompson, The glucose dependence of Akt-transformed cells can be reversed by pharmacologic activation of fatty acid beta-oxidation, Oncogene 24 (2005) 4165–4173.
[50] C.D. Simpson, K. Anyiwe, A.D. Schimmer, Anoikis resistance and tumor metastasis, Canc. Lett. 272 (2008) 177–185.
[51] Z.T. Schafer, A.R. Grassian, S. Loling, J. Zhenyang, G.H. Zachary, H.Y. Irie, G. Sizhen, P. Pere, J.S. Brugge, Antioxidant and oncogene rescue of metabolic defects caused by loss of matrix attachment, Nature 461 (2009) 109.
[52] A.E. Li, H. Ito, Rovira II, K.S. Kim, K. Takeda, Z.Y. Yu, V.J. Ferrans, T. Finkel, A role for reactive oxygen species in endothelial cell anoikis, Circ. Res. 85 (1999) 304–310.
[53] P. Chiarugi, From anchorage dependent proliferation to survival: lessons from redox signalling, IUBMB Life 60 (2008) 301–307.
[54] S. Reuter, S.C. Gupta, M.M. Chaturvedi, B.B. Aggarwal, Oxidative stress, inflammation, and cancer: how are they linked? Free Radical Biol. Med. 49 (2010) 1603–1616.
[55] B. Halliwell, Oxidative stress and cancer: have we moved forward? Biochem. J. 401 (2007) 1–11.
[56] Z.T. Schafer, A.R. Grassian, L. Song, Z. Jiang, Z. Gerhart-Hines, H.Y. Irie, S. Gao, P. Puigserver, J.S. Brugge, Antioxidant and oncogene rescue of metabolic defects caused by loss of matrix attachment, Nature 461 (2009) 109–113.
[57] K. Ishikawa, K. Takenaga, M. Akimoto, N. Koshikawa, A. Yamaguchi, H. Imanishi, K. Nakada, Y. Honma, J. Hayashi, ROS-generating mitochondrial DNA mutations can regulate tumor cell metastasis, Science 320 (2008) 661–664. New York, NY.
[58] F. Weinberg, R. Hamanaka, W.W. Wheaton, S. Weinberg, J. Joseph, M. Lopez, B. Kalyanaraman, G.M. Mutlu, G.R. Budinger, N.S. Chandel, Mitochondrial metabolism and ROS generation are essential for Kras-mediated tumorigenicity, Proc. Natl. Acad. Sci. U. S. A. 107 (2010) 8788–8793.
[59] K.E. Wellen, C.B. Thompson, Cellular metabolic stress: considering how cells respond to nutrient excess, Mol. Cell. 40 (2010) 323–332.